

Optimization of electrolyte and carbon conductor for dilithium terephthalate organic batteries

Ji-Eun Lim and Jae-Kwang Kim[†]

Department of Solar & Energy Engineering, Cheongju University, Cheongju, Chungbuk 28503, Korea

(Received 1 June 2018 • accepted 15 September 2018)

Abstract—Organic batteries are attractive alternatives to conventional inorganic batteries because of their low cost, biodegradation, and renewability, and their consequent environmental friendliness. We investigated the influence of carbon conductors and electrolytes in organic batteries using dilithium terephthalate ($\text{Li}_2\text{C}_8\text{H}_4\text{O}_4$). The synthesized dilithium terephthalate has well-grown crystallinity and non-uniform shaped particles without impurities. The dilithium terephthalate-based battery shows good electrochemical properties with a LiTFSI/TEGDME electrolyte and graphene as the carbon conductor in an organic electrode. The results are ascribed to the high lithium transference number of LiTFSI/TEGDME and the high electrical conductivity of graphene.

Keywords: Dilithium Terephthalate, Carbon Conductor, Electrolyte, Organic Batteries

INTRODUCTION

Portable electronic devices, electric vehicles, and hybrid electronic vehicles require energy storage capabilities to provide power, and lithium-ion batteries are mostly used in these systems due to their high rate-capability, long life cycle, and high energy output [1,2]. Lithium-ion batteries comprise an electrode, electrolyte, and separator, and electrode materials primarily determine the specific capacity, energy density, and cost of the batteries. Currently, inorganic materials are widely used as standard electrodes in commercial lithium-ion batteries. However, with the expansion of the lithium-ion battery market, the inorganic battery system faces issues regarding the resource limit, environmental impact, and recycling.

Organic electrode materials are a promising alternative, which can replace inorganic systems because they are environmentally friendly, cheap, abundant, and recyclable. Moreover, these materials can be synthesized from renewable resources, such as biomass, through eco-efficient processes, and do not require high-temperature annealing for good phase purity and crystallinity. Therefore, a low CO_2 footprint is expected in comparison to inorganic materials. Great efforts for the development of organic batteries have been made on organosulfur compounds, carbonyl compounds, and radical compounds [3-7]. Although the organic electrode has attractive characterization properties, it still incurs problems such as high self-discharge and low electrical conductivity, resulting in poor performance and fast decay during cycling [8,9]. Further, optimization of the composite material of the electrode and electrolyte in organic batteries is required for advantageous electrochemical properties.

In this study, we investigated the influence of the electrolyte and carbon conductor in the electrode on enhancing the electrochemical properties of organic batteries. The organic material entering the

organic battery was the carbonyl-based compound dilithium terephthalate ($\text{Li}_2\text{C}_8\text{H}_4\text{O}_4$), as carbonyl-based compounds can increase the theoretical capacity by modifying the structure. The capacity of the lithium terephthalate electrode is close to the theoretical capacity of 300 mAh g^{-1} , but the reversible capacity decays sharply, which leads to problems in the aforementioned organic electrode, such as low electrical conductivity and solubility in organic electrolytes [10-12]. To enhance the electrochemical properties of the $\text{Li}_2\text{C}_8\text{H}_4\text{O}_4$ organic battery, the influence of the electrolyte and carbon conductor should be investigated without considering the design of the electrode material. Carbon black and graphene were used as the conductor material, and 1 M LiPF_6 in EC/DMC and 1 M LiTFSI in TEGDME were used as the electrolyte to compare the performance. A carbon conductor was chosen because carbon black has a spherical morphology, whereas graphene has a layer morphology. The graphene of layer form has a higher conductivity ($\sim 10^7 \text{ S/m}$) with lower resistivity because of its thin two-dimensional morphology, compared to the carbon black ($\sim 10^5 \text{ S/m}$) of spherical form. The two electrolytes used are low-viscosity and high-viscosity liquid electrolytes. The viscosity of electrolyte affects stability of organic electrode [13,14]. The use of graphene as the carbon conductor and LiTFSI/TEGDME as the electrolyte, in combination, shows improved electrochemical properties.

EXPERIMENTAL

To synthesize lithium terephthalate ($\text{Li}_2\text{C}_8\text{H}_4\text{O}_4$), 1.66 g tertralic acid is slowly dissolved in 50 ml ethanol at 80 °C for 12 h, in a solution of 0.9 g of $\text{LiOH}\cdot\text{H}_2\text{O}$ in 25 ml distilled water. Next, the obtained solution is centrifuged and dried in a vacuum at 80 °C for 12 h. A white powder of $\text{Li}_2\text{C}_8\text{H}_4\text{O}_4$ is finally obtained. The structure and chemical composition of the prepared samples were observed using X-ray diffraction (XRD, Ulvac-PHI PHI Quantera-II) and Fourier transform infrared spectroscopy (FT-IR, BRUKER OPTIK GMBH IFS 66/S). Elemental mapping was observed using scanning elec-

[†]To whom correspondence should be addressed.

E-mail: jaekwang@cju.ac.kr

Copyright by The Korean Institute of Chemical Engineers.

tron microscopy (SEM), utilizing a Nanonova 230 scanning electron microscope (FEI, USA). The lithium ion transference number (t_{Li^+}) was estimated using the DC polarization method with Bruce and Vincent correction. The working electrodes were prepared with two types of carbon black (or graphene) of 40 wt%, with 50 wt% $\text{Li}_2\text{C}_8\text{H}_4\text{O}_4$ active material and 10 wt% polyvinylidene fluoride (PVDF) binder on Cu foil. The coin-type cell comprises the working electrodes, lithium metal counter electrode, and Celgard®2300 separator in an argon filled glove box. To facilitate comparison of electrochemical characterization, two different types of electrolytes, 1 M lithium hexafluorophosphate (LiPF_6) in ethylene carbonate (EC)/dimethyl carbonate (DMC) (1 : 1 v/v, PanaX. Etec Co.) and 1 M bis(trifluoromethane)sulfonimide lithium salt (LiTFSI) in tetraethylene glycol dimethyl ether (TEGDME) were used. Electrochemical performance tests were conducted using an automatic galvanostatic charge-discharge unit (WBCS3000 battery cycler), between 0.5 and 3.0 V, at room temperature.

RESULTS AND DISCUSSION

The structural and chemical nature of the white powder synthesized by $\text{LiOH}\cdot\text{H}_2\text{O}$ and tertralic acid was measured by XRD and FT-IR. Fig. 1(a) shows the XRD pattern of $\text{Li}_2\text{C}_8\text{H}_4\text{O}_4$; the XRD data can provide information on the structure, composition, and physical properties of the materials. The phase of the synthesized material was confirmed to be a monoclinic crystal system through the JCPDS file (no. PDF#52-2147) of dilithium terephthalate, which showed it to be devoid of an impurity phase caused by an undesirable reaction [10]. The diffraction lines can be assigned to the $P2_1/c$ space group, and the intensity is high due to the well-formed crystallinity in the particle. The inset figure shows the scanning electron microscopy (SEM) images of pristine dilithium terephthalate. It can be clearly seen that the $\text{Li}_2\text{C}_8\text{H}_4\text{O}_4$ consists of non-uniformly shaped particles, with the maximum size of around 20 μm . The FT-IR absorption spectrum of dilithium terephthalate is shown in Fig. 1(b). The band at $\sim 526 \text{ cm}^{-1}$ indicates the presence of the O-Li ion bond. The wavenumber at $\sim 1,391$ and $\sim 1,578 \text{ cm}^{-1}$ can be attributed to the COO^- group [12]. Fig. 2 shows the electrochemical mechanism of $\text{Li}_2\text{C}_8\text{H}_4\text{O}_4$ for storing two Li cations per formula

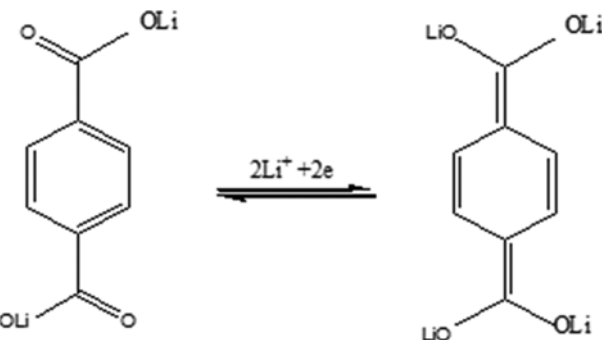


Fig. 2. Schematic for Li-ion bonding and de-bonding in $\text{Li}_2\text{C}_8\text{H}_4\text{O}_4$.

unit, involving a breaking aromatic p-bond in the benzenoid ring. When charging and discharging, $\text{Li}_2\text{C}_8\text{H}_4\text{O}_4$ bonds and de-bonds with two Li^+ ions in two carbonyl groups.

The effect of the electrolytes and carbon conductors was investigated in Fig. 3, with charge-discharge performance of $\text{Li}_2\text{C}_8\text{H}_4\text{O}_4$ in a cut-off range of 0.5–3 V at 0.1 C. Fig. 3(a) shows the second charge-discharge curves, in which different liquid electrolytes are used for an electrode using carbon black as the conductor material. The charge and discharge capacity when using LiPF_6 in EC/DMC is 83.6 and 93.5 mAh g^{-1} , respectively, while that when using LiTFSI/TEGDME is 110.6 and 183.9 mAh g^{-1} , respectively. Fig. 3(b) shows the charge-discharge curves in which different electrolytes are used for an electrode containing graphene as the carbon conductor. The charge and discharge capacity when using LiPF_6 in EC/DMC is 131.3 and 179.3 mAh g^{-1} , respectively, and that when using LiTFSI/TEGDME is 370.8 and 564.0 mAh g^{-1} , respectively. In Fig. 3(a) and (b), a plateau voltage of 1.1 V and 0.8 V is shown in the charge-discharge graph, and it is confirmed that the capacity is increased when LiTFSI/TEGDME is added to the cell. The higher capacity of LiTFSI/TEGDME is ascribed to the lithium transference number ($t_{Li^+} \sim 0.6$) being higher than that of LiPF_6 in EC/DMC ($t_{Li^+} \sim 0.36$), and the high viscosity prevents dissolution of the active material [13,14]. The lithium transference number is an important factor for the characterization of rechargeable lithium ion battery electrolytes because it represents the fraction of current carried

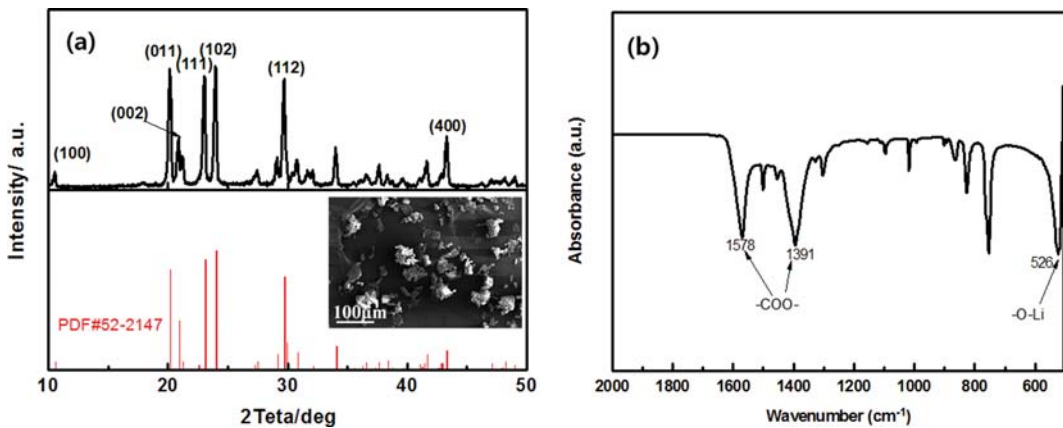


Fig. 1. (a) XRD pattern of $\text{Li}_2\text{C}_8\text{H}_4\text{O}_4$. The scanning electron micrograph of $\text{Li}_2\text{C}_8\text{H}_4\text{O}_4$ corresponds to the XRD (inset) and (b) FT-IR spectra of $\text{Li}_2\text{C}_8\text{H}_4\text{O}_4$.

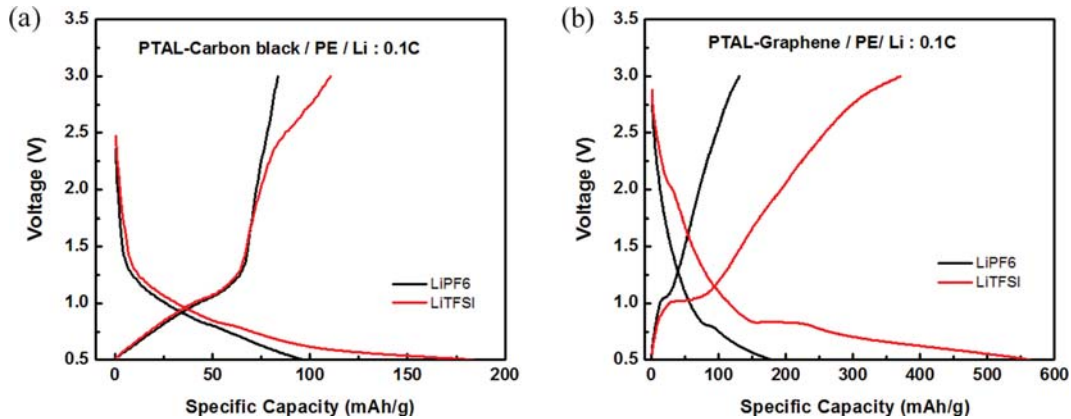


Fig. 3. (a) Charge and discharge curves of $\text{Li}_2\text{C}_8\text{H}_4\text{O}_4$ using super-p as the conductive material, comparing 1 M LiPF_6 in EC/DMC and 1 M LiTFSI in TEGDME as the electrolytes. (b) Charge and discharge curves of $\text{Li}_2\text{C}_8\text{H}_4\text{O}_4$ using graphene as the conductive material, comparing 1 M LiPF_6 in EC/DMC and 1 M LiTFSI in TEGDME as the electrolytes.

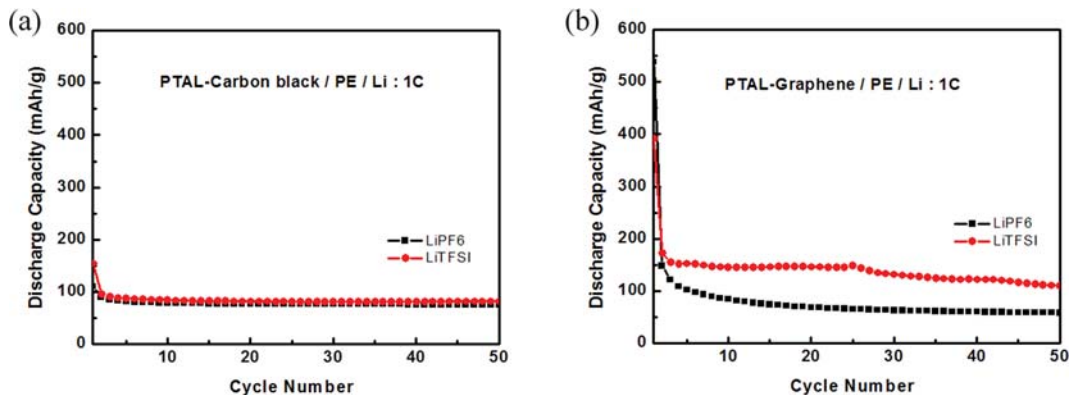


Fig. 4. (a) Cycle performance of $\text{Li}_2\text{C}_8\text{H}_4\text{O}_4$ using super-p as the conductive material, comparing 1 M LiPF_6 in EC/DMC and 1 M LiTFSI in TEGDME as the electrolytes. (b) Cycle performance of $\text{Li}_2\text{C}_8\text{H}_4\text{O}_4$ using graphene as the conductive material, comparing 1 M LiPF_6 in EC/DMC and 1 M LiTFSI in TEGDME as the electrolytes.

by lithium ions. The higher value is beneficial to achieve high capacity on the organic battery. In addition, the results show that the capacity of the cell containing the graphene conductor was higher than that of the one containing carbon black. This is because graphene is more conductive than carbon black, making migration of Li^+ ions easier with rapid electron transfer into electrode. It was confirmed that the discharge capacity of the cell containing the TEGDME electrolyte was dramatically increased in the $\text{Li}_2\text{C}_8\text{H}_4\text{O}_4$ electrode using the graphene conductive material.

Fig. 4 shows the cycle stability of the organic anode with different electrolytes and carbon conductors. The cycle performance was measured at a 1 C-rate in the 0.5–3.0 V cut-off range, to mitigate the effects of carbon materials on lithium ion storage ($<0.5 \text{ V}$) [15]. Since a solid electrolyte interface (SEI) layer is formed in the first cycle, the capacity drops sharply from the first cycle to the second cycle in Fig. 4(a) and (b) [16]. In Fig. 4(a), the second discharge capacity of the cell containing the LiPF_6 in EC/DMC is 88.9 mAh g^{-1} and that of the cell containing $\text{LiTFSI}/\text{TEGDME}$ is 95.4 mAh g^{-1} . After 50 cycles, the discharge capacities are 75.2 and 81.9 mAh g^{-1} for carbon black as carbon conductor, respectively, and the capacity retention rate is 84.6 and 85.8% , respectively. In Fig. 4(b),

the second discharge capacity of the cell containing the LiPF_6 in EC/DMC is 147.6 mAh g^{-1} , and second discharge capacity with the $\text{LiTFSI}/\text{TEGDME}$ is 173.1 mAh g^{-1} . After 50 cycles, the discharge capacities are 57.7 and 109.5 mAh g^{-1} , respectively, and the capacity retention ratios are 39 and 63.3% , respectively. The capacity retention of carbon black is better than that of graphene. With the graphene support, leading to serious capacity fading on second cycles, because the $\text{Li}_2\text{C}_8\text{H}_4\text{O}_4$ electrode incurred agglomeration during Li ion intercalation and deintercalation [17]. Further, the capacity of the battery using the TEGDME-based electrolyte was superior to that of the battery using the liquid electrolyte.

CONCLUSION

We investigated the influence of the electrolyte and carbon conductor in the $\text{Li}_2\text{C}_8\text{H}_4\text{O}_4$ organic electrode to enhance the electrochemical properties of organic batteries. Carbon black and graphene were selected as the carbon conductors in the electrodes, and LiPF_6 in EC/DMC and $\text{LiTFSI}/\text{TEGDME}$ was compared. It was confirmed that the cells using graphene as the conductor material had improved capacity, but the capacity retention was lower than that

of carbon black. Considering the electrolyte, LiTFSI/TEGDME, with a high viscosity, significantly improved the electrochemical properties compared to the conventional liquid electrolyte because LiTFSI/TEGDME has a higher lithium transference number and prevents the dissolution of the organic electrode.

REFERENCES

1. N. Nitta, F. Wu, J. T. Lee and G. Yushin, *Mater. Today*, **18**, 252 (2015).
2. V. Etacheri, R. Marom, R. Elazari, G. Salitra and D. Aurbach, *Energy Environ. Sci.*, **4**, 3243 (2011).
3. Y. Kiya, J. Henderson, G. Hutchison and H. Abrun, *J. Mater. Chem.*, **17**, 4366 (2007).
4. G. Yang, Y. Zhang, Y. Huang, M. Shakir and Y. Xu, *Phys. Chem. Chem. Phys.*, **18**, 31361 (2016).
5. T. Schon, B. McAllister, P. Li and D. Seferos, *Chem. Soc. Rev.*, **45**, 6345 (2016).
6. D. Nevers, F. Brushett and D. Wheeler, *J. Power Sources*, **352**, 226 (2017).
7. J. K. Kim, *J. Power Sources*, **242**, 683 (2013).
8. Y. Xu, M. Zhou and Y. Lei, *Mater. Today*, **21**, 60 (2017).
9. Y. Liang, Z. Tao and J. Chen, *Adv. Energy Mater.*, **2**, 742 (2012).
10. Q. Yu, D. Chen, J. Liang, Y. Chu, Y. Wu, W. Zhang, Y. Li, L. Li and R. Zeng, *RSC Adv.*, **4**, 59498 (2014).
11. Q. Deng, J. Xue, W. Zou, L. Wang, A. Zhou and J. Li, *J. Electroanal. Chem.*, **761**, 74 (2016).
12. M. Armand, S. Grigeon, H. Vezin, S. Laruelle, P. Ribière, P. Poizot and J.-M. Tarascon, *Nat. Mater.*, **8**, 120 (2009).
13. G. Elia, J. B. Park, Y. K. Sun, B. Scrosati and J. Hassoun, *ChemElectroChem.*, **1**, 47 (2014).
14. J. K. Kim, A. Matic, J. H. Ahn and P. Jacobsson, *RSC Adv.*, **2**, 9795 (2012).
15. Y. Tang, L. Liu, H. Zhao, D. Jia and W. Liu, *J. Mater. Chem. A.*, **4**, 2089 (2016).
16. S. Zhang, *J. Power Sources*, **162**, 1379 (2006).
17. J. Cheng and J. Du, *CrystEngComm.*, **14**, 397 (2012).